Available online at www.sciencedirect.com
ScienceDirect
Journal of the European Ceramic Society 30 (2010) 1007–1014
www.elsevier.com/locate/jeurceramsoc

Microstructural evolution during the infiltration of boron carbide with molten silicon

Shmuel Hayun, Amir Weizmann, Moshe P. Dariel, Nahum Frage *

Department of Materials Engineering, Ben-Gurion University of the Negev, P.O. Box 653, Beer-Sheva 84105, Israel

Received 18 May 2009; received in revised form 3 September 2009; accepted 18 September 2009
Available online 5 November 2009

Abstract

The previously reported model that accounts for the formation of the core-rim structure in reaction-bonded boron carbide composites (RBBC) is expanded and validated by additional experimental observations and by a thermodynamic analysis of the ternary B–C–Si system. The microstructure of the RBBC composites consists of boron carbide particles with a core-rim structure, β-SiC and some residual silicon. The SiC carbide particles have a polygonal shape in composites fabricated in the presence of free carbon, in contrast to the plate-like morphology when the initial boron carbide is the sole source of carbon. In the course of the infiltration process, the original B_4C particles dissolve partly or fully in molten silicon, and a local equilibrium is established between boron carbide, molten silicon and SiC. Overall equilibrium in the system is achieved as a result of the precipitation of the ternary boron carbide phase $B_{12}(B,C,Si)_3$ at the surface of the original boron carbide particles and leads to the formation of the rim regions. This feature is well accounted for by the "stoichiometric saturation" approach, which takes into account the congruent dissolution of B_4C particles. The SiC phase, which precipitates form the silicon melt adopts the β-allotropic structure and grows preferably as single plate-like particles with an $\{1\,1\,1\}_\beta$ habit plane. The morphology of the SiC particles is determined by the amount of carbon available for their formation.

Keywords: Boron carbide; SiC; RBBC; Core-rim structure; Morphology

1. Introduction

Reaction-bonded boron carbide (RBBC) is the product of the infiltration process of a green boron carbide compact with molten silicon.[1–6] Infiltration can take place in or without the presence of free carbon, giving rise to different morphologies of the silicon carbide particles.[3] Silicon carbide particles have a polygonal shape in the composites, fabricated in the presence of free carbon and a plate-like morphology when boron carbide is the sole source of carbon. Lately, it was reported that the plate-like β-SiC particles provide improved mechanical properties to the composites.[7] The core-rim structure of the boron carbide particles in RBBC has been described previously.[3] The formation of the rim region with composition that corresponds to the ternary $B_{12}(B,C,Si)_3$ phase, was attributed to the dissolution-precipitation process.[3,8–10] The core-rim structure is of common occurrence in composites, fabricated by powder metallurgy, when liquid and solid phases are involved in the evolution of the microstructure.

The presence of the core-rim structure was observed in metal–ceramic systems containing complex carbide or carbonitride phases partly soluble in a liquid metal[11–13] and in metal–metal tungsten-based composites after liquid phase sintering.[14,15] Different mechanisms have been put forward in the literature in order to explain this microstructural feature.[11,14,16–22] The formation of the core-rim structure in a solid–liquid system is attributed to the partial dissolution of original particles in the liquid and precipitation of a new solid phase at the surface of the initial particles. The driving force for continuous mass transfer through the liquid phase may be attributed to the difference in particle size ("Ostwald ripening" mechanism) or to the composition change that takes place in the solid following its dissolution and subsequent precipitation with an altered composition.

The Ostwald ripening mechanism does not always lead to the formation of the core-rim structure. It does only if the composition of the solid phase undergoes a change during the dissolution process[14,16] or if a component of the liquid finds its

* Corresponding author. Fax: +972 8 647941.
E-mail address: nfrage@bgu.ac.il (N. Frage).

0955-2219/$ – see front matter © 2009 Elsevier Ltd. All rights reserved.
doi:10.1016/j.jeurceramsoc.2009.09.021

way in the newly precipitated ceramic phase.[17,18] Most often a change of the composition of the original solid phase involves a solid phase diffusion process, the rate of which is generally low and is unlikely to take place, at least, in ceramic phases with strong covalent bonds. The incorporation of a component of the liquid phase into the precipitated ceramic phase is the more likely process whereby a rim region is formed around the original ceramic particles. Such process has been observed to take place in the course of the microstructural evolution in TiC-steel composites[19] and in silicon infiltrated reaction-bonded boron carbide.[3] The formation of a layered rim region was discussed by Chen et al.[11] The authors suggested that the inner layer is formed as a result of the precipitation of a new phase under quasi-isothermal conditions, as long as the original ceramic phase is in contact with the liquid. The outer layer is formed during the solidification process with decreasing solubility of the components in the liquid. The inner layer is formed as a result of congruent or stoichiometric ceramic phase dissolution in the liquid and its re-precipitation with a different composition, as determined by equilibrium requirements. Chen et al.[11] also discarded the alternative option of a solid-state diffusion induced formation of the inner layer because the diffusion rate in the covalently bonded solid is too low.

A similar mechanism for the evolution of a core-rim structure has been discussed in connection with various geological systems. At solid solution-aqueous solution (SS-AS) interfaces the composition of a solid phase remains invariant due to kinetic restrictions[20–22] and a partial equilibrium between a liquid and a multi-component solid phase, referred to as "stoichiometric saturation"[23] is established.

In the present study the mechanism of microstructural evolution during RBBC composites fabrication with and without the presence of free carbon, namely the core-rim structure formation and the different morphologies of β-SiC, formed as a result of the interaction of liquid Si with boron carbide or with free carbon, are discussed based on the previous experimental observations and on the results of a thermodynamic analysis of the ternary B–Si–C system

Table 1
Details of the samples infiltrated with liquid Si.

Sample type	Average particle size, μm	Carbon addition
A	100	No
B	100	5 wt.%
C	5	No

2. Experimental procedure

Three sets of samples denoted A, B and C (Table 1) were fabricated from commercial boron carbide powder (Mudanjiang abrasives and grinding tools co., People Republic of China, 95% purity). The specific properties of this powder were reported in our previous work.[24] Preforms of 20 mm diameter and 3 mm *height* were uniaxially compacted (25 MPa). Five wt. % free carbon was added to the porous preforms of type-B samples by infiltration with an aqueous sugar solution (50:50). The infiltrated preforms were dried and heat treated at 773 K in order to pyrolize the sugar. The preforms were infiltrated with silicon (Alfa Aesar, 99.9999%) in a vacuum furnace (10^{-5} torr) at 1723 K for 15 min. The infiltration was carried out by placing an appropriate amount of silicon lump on the top of the porous preforms.

The microstructure of the samples was studied by scanning electron microscopy (SEM, JEOL-35) in conjunction with an energy-dispersive spectrometer (EDS) and by transmission electron microscopy (TEM, JEOL-2010). The samples for the SEM characterization were prepared using a standard metallographic procedure that included a last stage of polishing by 1 μm diamond paste. In order to put in evidence the difference between the rim and core regions, the samples underwent electro-chemical etching in a KOH solution. The samples for TEM examination were prepared as follows: 1 mm thick foils were cut using a 0.4 mm thick diamond saw and ground down to 500 μm. Disks of 3 mm diameter were drilled with a copper drill pipe and 40 μm diamond paste, ground down to 70 μm thickness, and polished to 30 μm thickness. The perforation stage was carried out using Gatan^{TM}-precision ion polishing system.

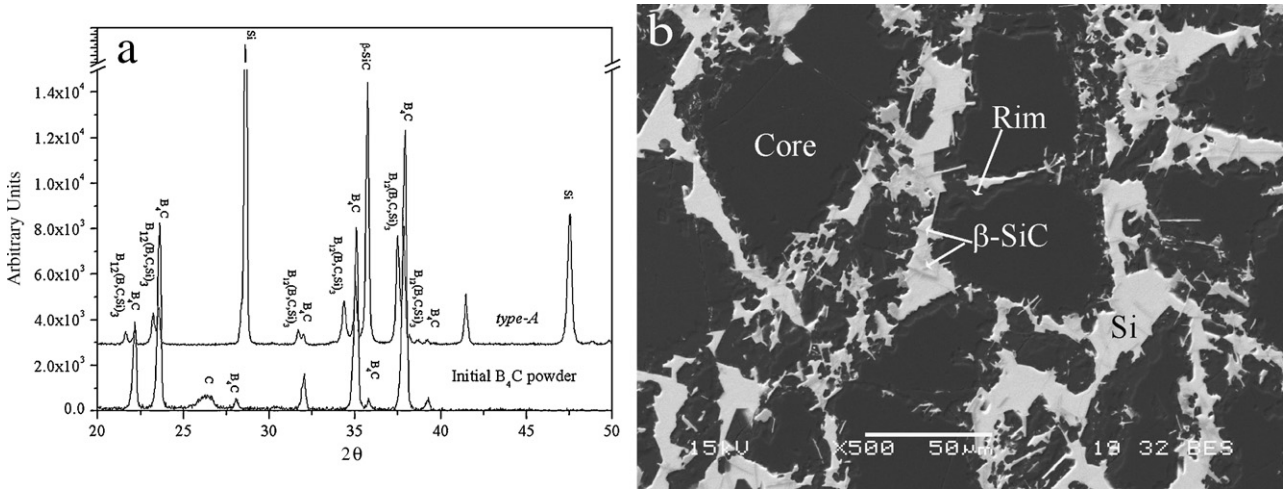

Fig. 1. (a) XRD pattern of the starting boron carbide powder and the *type-A* composite, (b) SEM micrograph (back scattered electrons) of *type-A* composite, the boron carbide particles have a core-rim structure of B_4C cores, surrounded by a 3–7 μm thick $B_{12}(B,C,Si)_3$ envelope.

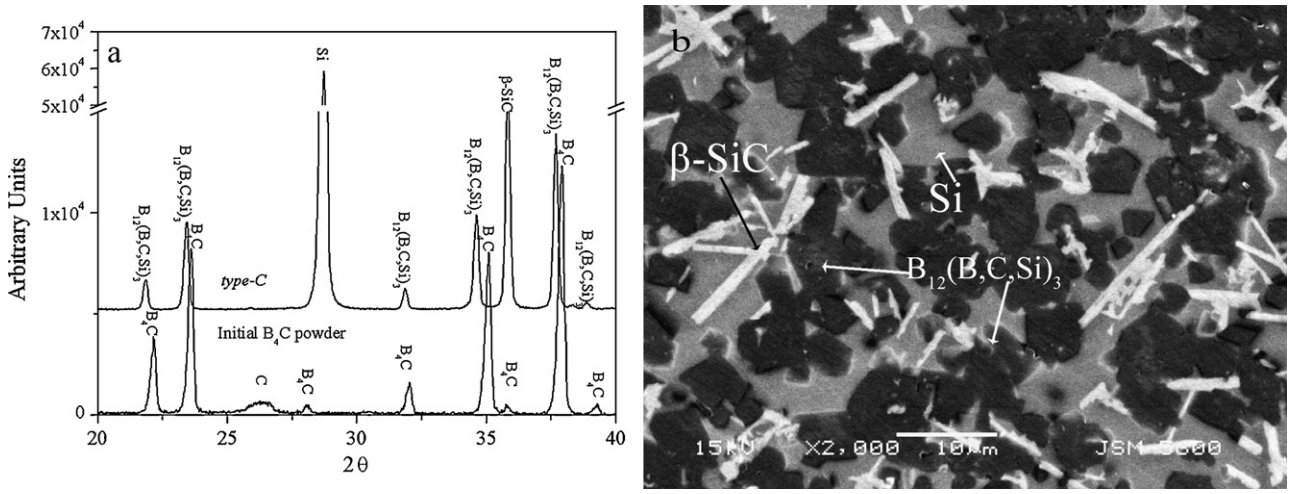

Fig. 2. (a) XRD plot of *type-C* composite, notice the total absence of the B_4C reflections. (b) SEM (secondary electrons) micrograph of *type-C* composite.

The phase composition and the structure of the samples was determined by X-ray diffraction (XRD), using a Rigaku RINT 2100 diffractometer with Cu Kα radiation. The scanning angle 2θ was increased in 0.02° steps.

3. Experimental observations

3.1. Core-rim structure of the boron carbide particles

According to the results of XRD analysis (Fig. 1a), the infiltrated *type-A and B* composites consist of two clearly distinct boron carbide patterns with different lattice parameters, β-SiC and residual silicon. The diffraction spectrum with the larger lattice parameter corresponds to the ternary $B_{12}(B,C,Si)_3$ compound.[25] The microstructure of the sample revealed the core-rim structure of the boron carbide particles, with B_4C cores being surrounded by a 3–7 μm thick $B_{12}(B,C,Si)_3$ envelope (Fig. 1b).

In the XRD patterns of *type-C* composites, which had been fabricated using compacted preforms consisting of 5 μm initial particles, only diffraction peaks corresponding to the $B_{12}(B,C,Si)_3$,SiC and Si components were observed. Noteworthy, the total absence of the initial boron carbide diffraction peaks, suggesting that the initial particles had completely transformed into the new $B_{12}(B,C,Si)_3$ phase. It is also noteworthy, that the average particle size of the newly formed ternary carbide phase was about the same as that of the initial boron carbide particles (Fig. 2). In our previous communication [3], the preforms had been also prepared from 5 μm size powder that had undergone, prior infiltration, an intermediate sintering treatment. During the sintering stage the boron carbide particles size increased to 10 μm and after infiltration the core-rim structure was observed.[3] According to Hayun et al.[26], the dissolution–precipitation process takes place at the initial stage (about 10 min) of the interaction between original boron carbide particles and molten silicon and generates a 5–7 μm thick rim that maintains a nearly constant thickness. The complete transformation of the *type-C* composite into the ternary carbide phase can be accounted for by the rim maintaining a thickness of the order of the initial powder size. In composites, fabricated form the partly sintered preforms and with an average grain size larger than 10 μm, some original boron carbide grains subsisted and was detected by XRD analysis along with the presence of the new formed ternary carbide.

3.2. The morphology of the silicon carbide particles

Two distinct morphologies of the β-SiC phase were observed in RBBC and are related to the carbon source. In the presence

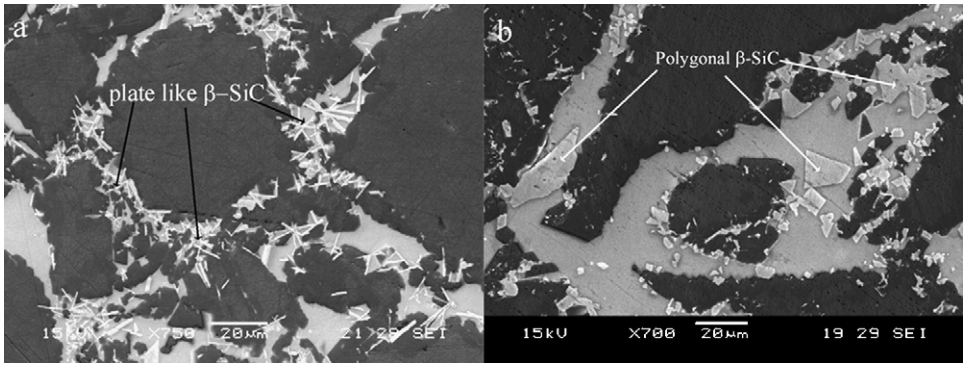

Fig. 3. SEM (secondary electrons) images of the bulk regions in the composites without (a) and with (b) free carbon addition.

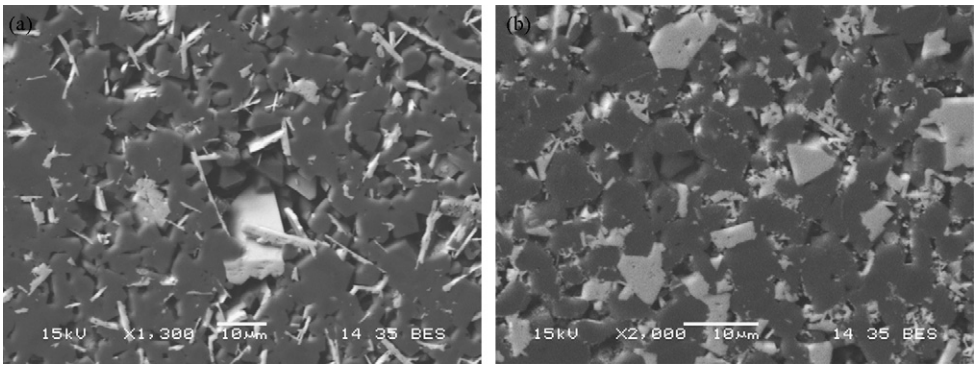

Fig. 4. SEM image of the chemical etched ($HF–NHO_3$) the bulk regions samples without (a) and with (b) free carbon addition. The morphology of the SiC phase is clearly apparent.

of free carbon in the boron carbide preform, β-SiC adopts a polygonal shape (Figs. 3b and 4b), while in the absence of free carbon, SiC particles display a plate-like shape (Figs. 3a and 4a).

The TEM micrograph of the polygonal β-SiC grain in the *RBBC* composite, fabricated in the presence of free carbon, revealed that this type of grains is built by mutually bonded plate-like particles (Fig. 5). The structure of the plate-like β-SiC particle is heavily twinned as is that of the plate-like β-SiC particles, in composites fabricated in the absence of free carbon addition (Fig. 6). A further structural analysis confirmed that the plate-like β-SiC preferably grows as a single plate with $\{1\,1\,1\}_\beta$ growth habit plane.

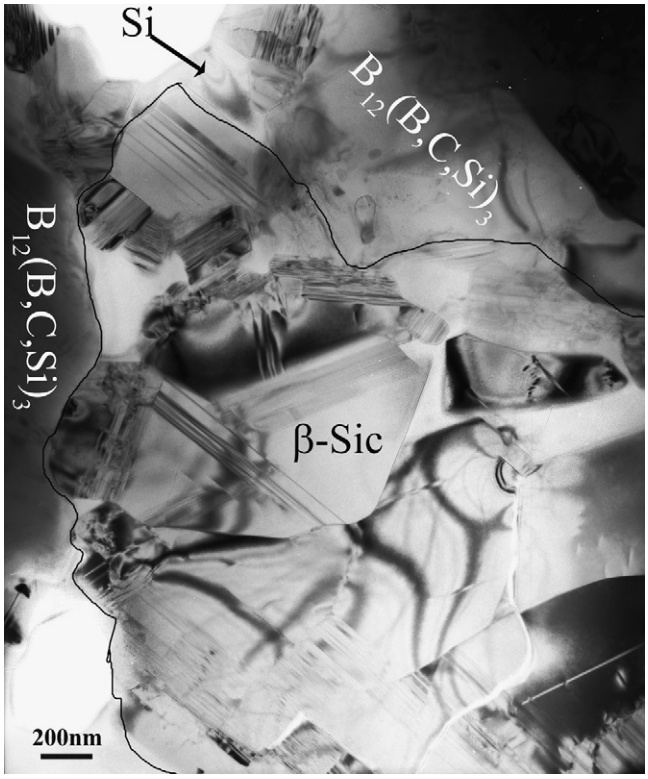

Fig. 5. TEM micrograph of polygonal β-SiC particles. These particles consist of several plate-like particles mutually bonded. The contour line marks the polygonal β-SiC particle.

4. Discussion

The formation of the core-rim structure of the original boron carbide particles has been discussed in a previous communication[3] and was attributed to the "Ostwald ripening" mechanism. However, this mechanism fails to explain the microstructure of *type-C* composite, fabricated from fine boron carbide particles, where most of the boron carbide particles transformed into the $B_{12}(B,C,Si)_3$ phase.

This experimental observation required the necessity for a different mechanism in order to explain the core-rim structure and the boron carbide transformation mechanism. We suggest that this mechanism is most likely identified with the above-mentioned "stoichiometric saturation" approach, which can be accounted for by a thermodynamic analysis of the B–C–Si system.

4.1. Thermodynamic analysis of the B–C–Si system

Analysis of phase equilibria in the B–C–Si system involves the description of the ternary $B_{12}(B,C,Si)_3$ carbide phase, which was treated as a solid solution of Si in boron carbide. Unfortunately, the information about the solubility of Si in boron carbide is very limited. According to Werheit et al.[27] and Telle[8] the maximal solubility of Si in boron carbide at 2323 K is about 2.5 at.%. Goujard et al.[28] has conducted a thermodynamic assessment of the B–C–Si system at 1400 K, without taking into account the formation of the ternary carbide phase. An attempt to take into account the silicon solubility in boron carbide was performed by Kasper,[29] who suggested that Si_2 units are incorporated in the linear chains of the boron carbide lattice.[27] This model allowed Kasper[29] to calculate relatively high temperatures isothermal sections of the ternary B–C–Si phase diagram and to achieve good agreement with the experimental results reported in.[8] In order to calculate the isothermal section at the infiltrating temperature, the thermodynamic parameters of solid and liquid solutions in the ternary B–C–Si system, in the present work, were taken form Kasper[29] and extrapolated to 1753 K. The isothermal section calculated using the Thermo-Calc software[30] is presented in Fig. 7 and is used for discussing the microstructural evolution in the RBBC composites. Initially, the porous boron carbide body with a green density of about 60% is fully infiltrated

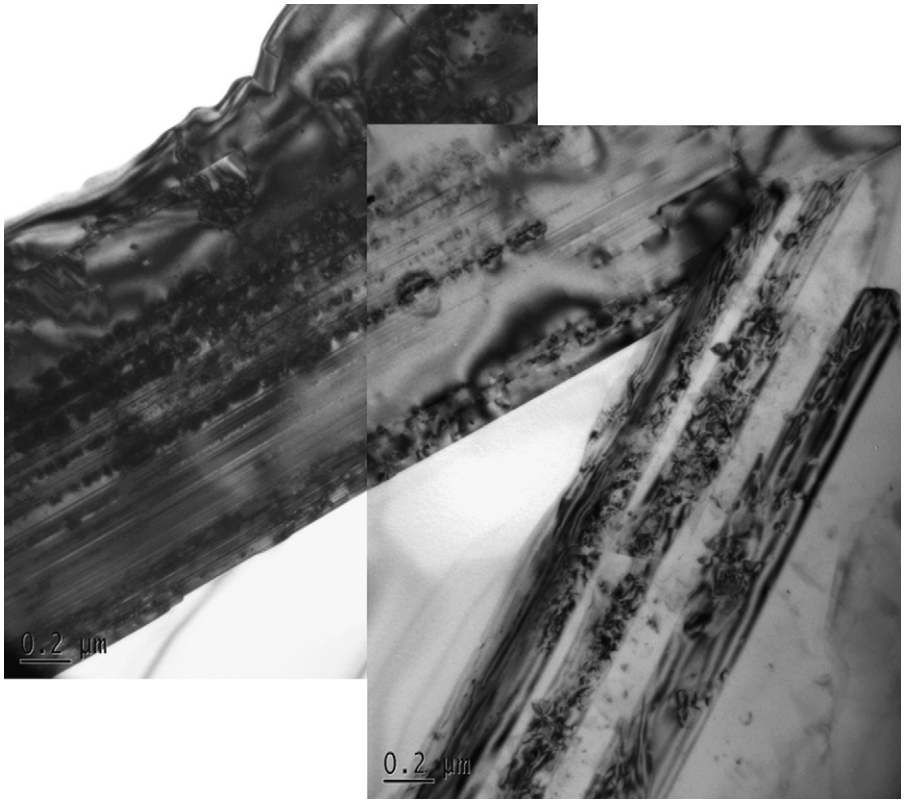

Fig. 6. TEM micrograph of plate-like β-SiC particles in samples in the absence of free carbon. These particles consist of stacks of twins.

with molten silicon. The nominal atomic starting composition of the system 63 at. % B, 16 at.% C and 21 at.% Si (before any interaction) corresponds to the point *A* in Fig. 7. This point lies on the dashed line, which connects the silicon corner of the isothermal section with the point corresponding to B_4C, namely to the boron-to-carbon ratio equal to 4. The point *A* is located within the three-phase region: Si–B–C liquid solution, SiC and $B_{12}(B,C,Si)_3$. Thus, if equilibrium conditions were achieved, all original boron carbide particles should convert into the new $B_{12}(B,C,Si)_3$ phase that contains a certain amount of silicon. Actually, the system does not reach equilibrium, because the new $B_{12}(B,C,Si)_3$ phase precipitates at the surface of the initial boron carbide particles, forms the rim region, which acts as a barrier and prevents the continuous dissolution of the boron carbide. As mentioned above, boron carbide does not change its composition during the dissolution stage, due to diffusion constrains and, therefore, initially only partial equilibrium between silicon melt and B_4C is established. The overall equilibrium conditions corresponding to the isothermal section (Fig. 7) are achieved when precipitation of the $B_{12}(B,C,Si)_3$ phase takes place. The compositions of the liquid for both the partial and the overall equilibrium as well as the driving force for the rim region formation may be estimated using the calculated isothermal

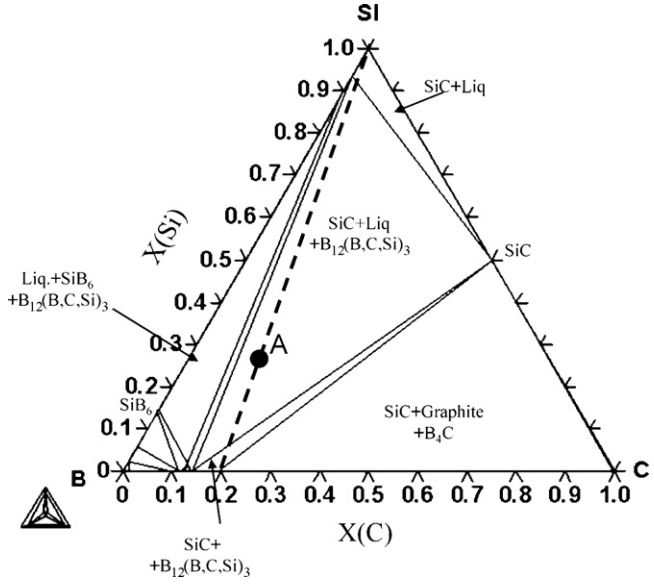

Fig. 7. Isothermal section of the B–C–Si phase diagram at 1753 K. The relevant two and three- phase regions are marked out in the isothermal sections.

4.2. Core-rim structure formation mechanism

Since boron carbide is a covalently bonded solid, its components diffuse at an extremely low rate, it dissolves, therefore, congruently, e.g. without any compositional changes. The boron concentration in the melt as a result of the congruent dissolution of boron carbide was calculated using thermodynamic data for the reaction $B_4C = 4[B] + [C]$, where the brackets denote the elements dissolved in liquid silicon. The calculated value for this partial equilibrium in the system is equal to 8.0 at.% B. At the same time, the boron content in the melt, which is in equilibrium with SiC and the ternary $B_{12}(B,C,Si)_3$ phase is about

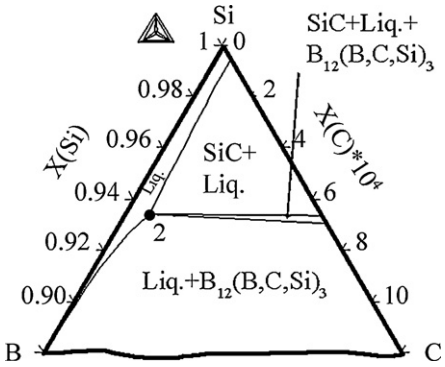

Fig. 8. The silicon rich corner of the isothermal section (1753 K) of the stable B–C–Si phase diagram.

6.6 at.% (Point 2 in the silicon rich corner of the isothermal section, Fig. 8). Thus, the congruent dissolution of boron carbide provides the required over-saturation for the ternary carbide formation. The precipitation of the silicon containing boron carbide phase $B_{12}(B,C,Si)_3$ enables the establishment of overall equilibrium conditions in the system. The precipitation of the ternary carbide phase takes place at the interface of the original boron carbide particles and leads to the formation of the rim regions. The precipitation stops only when the liquid reaches the new equilibrium composition corresponding to the point 2 in Fig. 8. The dissolution–precipitation process continues as long as the liquid is in contact with the original boron carbide particles.

The driving force for the "stoichiometric saturation" can be estimated on the basis of the difference in the solubility of boron in molten silicon, in equilibrium with B_4C and with the $B_{12}(B,C,Si)_3$ phase, respectively. The part of the isothermal section close to the point B corresponding to the ternary carbide phase is presented in Fig. 9. The exact composition of this phase is $B_{12}C_{1.99}Si_{0.037}$.

Partial equilibrium between the liquid, B_4C and SiC is reached when 8 at.% boron is dissolved in the liquid. The solubility of B in molten silicon in equilibrium with $B_{12}(B,C,Si)_3$ and SiC (point 2, Fig. 8) is about 6.6 at.%. Taking into account

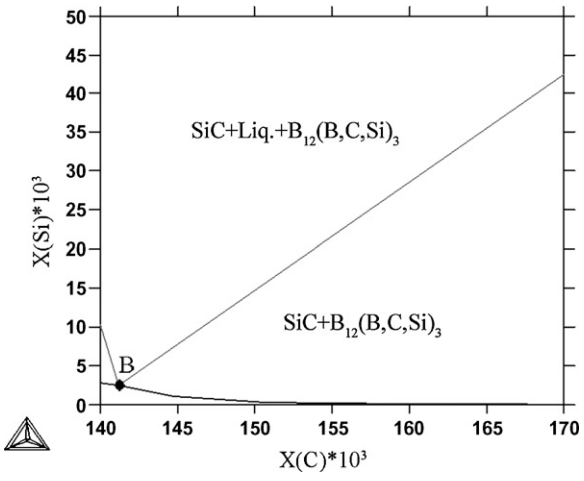

Fig. 9. Part of the isothermal section (1753 K) close to the point B corresponding to the composition of the ternary carbide phase.

Table 2
The activities the components of ternary phase calculated using the Thermo-[30] Calc Software.

Component	Component activity in B_4C (a_i^I)	Component activity in $B_{12}(B,C,Si)_3$ (a_i^{II})
C	0.0205	0.0202
B	0.2107	0.1789
Si	–	0.9

the composition of the ternary carbide and values of the activities (a_i^I) of its components (Table 2), the difference in the free energy of formation per 4 moles of boron can be calculated as

$$\Delta G^{II}_{formation}(B_4C_{0.667}Si_{0.012}) - \Delta G^{I}_{formation}(B_4C) = RT\ln\frac{(a_B^I)^4(a_C^I)}{(a_B^{II})^4(a_C^{II})^{0.667}(a_{Si}^{II})^{0.012}} = -9166\,\text{J/mole} \quad (1)$$

For comparison, the driving force for Ostwald ripening process was also estimated. According to Gibbs–Thompson, the change of the chemical potential $\Delta\mu$ of spherical particles relative to a flat interface as a function of particle size may be expressed as

$$\Delta\mu = -V_m\frac{2\gamma_{ls}}{r} \quad (2)$$

where V_m and γ_{ls} are the molar volume and the liquid–solid interface energy, r is the particle radius. Assuming that $\gamma_{ls} = 0.02$ J/mole[31] and molar volume of boron carbide $V_m = 2.19\times10^{-5}$ m^3/mole, the change of the chemical potential for type A, B, and C composites, as the average particle size varied from 1 to 100 μm is in the -0.576 to -8.76×10^{-3} J/mole range. The driving force for the "stoichiometric saturation" is significantly higher than that for the Ostwald ripening process. Thus, in the boron carbide-silicon system, the "stoichiometric saturation" is the most likely mechanism that stands behind the core-rim structure formation.

4.3. Morphology of SiC particles in the reaction-bonded composites

According to the experimental observation the morphology of the new formed β-SiC phase depends on the carbon source. In the composites fabricated with free carbon additions, polygonal shape SiC particles were observed, while in the composite where only boron carbide was the source of the carbon, most of β-SiC particles have a plate-like shape. It was also confirmed by TEM analysis that in both cases the SiC particles consist of a single plate with $\{1\,1\,1\}_\beta$ growth habit plane.

The mechanism of the reaction between liquid silicon and free carbon and the morphology of a new formed SiC phase has been widely discussed.[32–37] Fitzer and Gadow[38] and Li and Hausner[34] have suggested a two-stage mechanism for the interaction. At an initial stage, carbon dissolves in liquid silicon and after that heterogeneous nucleation and growth of a two dimensional continuous β-SiC layer on the carbon surface takes place. When the thickness of the β-SiC layer on the graphite interface

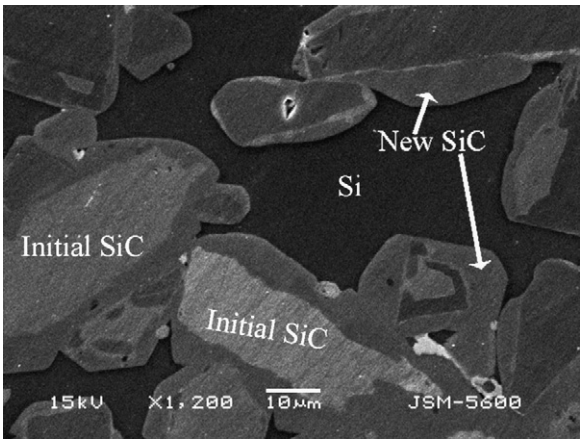

Fig. 10. SEM micrograph (secondary electrons) of RBSC composite. The composite was fabricated using an aqueous sugar solution as a source of free carbon. The new SiC layer precipitates on the initial SiC particles.

reaches several micrometers, the growth rate slows down and further increase in the layer thickness is controlled by solid-state diffusion. The β-SiC phase usually grows in plate-like shape and displays a strong anisotropic nature (twins and stacking faults develop only on one set of (1 1 1) planes. This feature was discussed by Moberlychan et al.[39] and was attributed to the growth rate being slower perpendicular to the planar surfaces.

The mechanism of the SiC formation during reaction bonding of the silicon carbide (RBSC) based composites was discussed by Pampuch et al.[40] and by Ness and Page.[33] It was suggested that similar to the system without initial SiC particles[36,38] at the initial stage of the interaction, carbon dissolves in the silicon melt. This dissolution provides a gradient of carbon concentration between the dissolution site and original SiC particles. Carbon diffuses to the surface of the SiC carbide particles and heterogeneous precipitation of newly formed SiC takes place. As a result of these processes, the specific microstructure of the RBSC composites is formed (Fig. 10). Moreover, Ness and Page[33] pointed out that the formation of the β-SiC phase in RBSC composites always starts as finger-like particles, which transform to the plate-like shape and finally broadening to the polygonal shape.

In reaction-bonded boron carbide composites fabricated in the presence of free carbon, two carbon sources are available for SiC formation. Moreover, as mentioned in Section 4.1, the solubility of carbon in the silicon melt at equilibrium with SiC is extremely low and does not depend on the carbon source. Nevertheless, in the vicinity of boron carbide particles the conditions for SiC formation are different from that for free carbon particles. As was discussed above, carbon and boron dissolve from boron carbide particles into the silicon melt and precipitation of SiC and $B_{12}(B,C,Si)_3$ phases takes place. The ternary carbide phase precipitates at the surface of the original boron carbide particles *via* a semi-coherent interface[3] and competes with SiC for the carbon atoms. The silicon carbide particles are nucleated within the melt only up to the stage at which the dissolution of boron carbide in the molten silicon raises the concentration of boron to its solubility limit. At this point, the ternary $B_{12}(B,C,Si)_3$ compound starts to precipitate at the carbide/melt interface and forms the rim regions. Further growth of the SiC nuclei is controlled by the available amount of carbon, which is significantly lower than in the vicinity of free carbon particles. These particles are commonly a product of the pyrolisis of carbon-rich organics, have a sponge-like structure with extremely high specific surface. Thus, a large number of SiC nuclei are formed at the carbon/liquid interface. These nuclei start to grow as plates, which coalesce and form the SiC/SiC grain boundaries within the polygonal SiC particle by the mechanism similar to that for the RBSC composites.

Based on the described above mechanisms of SiC formation, we suggest that the available amount of carbon is a key factor that determines the morphology of the β-SiC phase. If only boron carbide is the carbon source, the amount of carbon is limited, the β-SiC particles adopt a plate-like shape (Figs. 3a and 4a.). If free carbon is present in the green body and other phases do not compete with SiC, most β-SiC particles achieve a polygonal shape (Fig. 3b and 4b).

5. Summary

The microstructure of reaction-bonded boron carbide composites (RBBC) consists of core-rimmed boron carbide particles, β-SiC and residual Si. The core-rim structure in the reaction-bonded boron carbide composites is due to the dissolution-precipitation process, most likely by the "stochiometric saturation" mechanism. In the course of the infiltration, molten silicon is saturated with boron and carbon and, as a consequence, a secondary equilibrium ternary boron carbide phase ($B_{12}(B,C,Si)_3$), containing some silicon, is formed along with SiC particles in the melt. The newly formed equilibrium phase, $B_{12}(B,C,Si)_3$, precipitates at the interface of the initial boron carbide particles and forms the rim regions. According to the TEM analysis, the β-SiC phase single plate-like particles precipitate form the silicon melt preferably with the $\{1\,1\,1\}_\beta$ habit plane. The available amount of carbon for SiC formation during the process stands behind the different morphology in the composites fabricated with and without free carbon additions.

Acknowledgments

The authors wish to thank Dr. L. Dilman for her assistance in sample preparation and Mis Landau P. for the TEM analysis.

References

1. Aghajanian, M. K., Morgan, B. N., Singh, J. R., Mears, J. and Wolffe, R. A., A new family of reaction bonded ceramics for armor applications. In *Ceramic Transactions, Ceramic Armor Material by Design*, ed. J. W. McCauley and A. Crowson. American Ceramic Society, Westerville, OH, 2001, pp. 527–539.
2. Taylor, K. M. and Palicka, R. J., *Dense carbide composite for armor and abrasives*. U. S. Patent No. 3,765,300, 1973.
3. Hayun, S., Frage, N. and Dariel, M. P., The morphology of ceramic phases in BxC–SiC–Si infiltrated composites. *J. Solid State Chem.*, 2006, **179**, 2875–2879.
4. Hayun, S., Frage, N., Dilman, H., Tourbabin, V. and Dariel, M. P., Synthesis of dense B_4C–SiC–TiB_2 composites. In *Ceramic Armor and Armor Systems II*, ed. E. Medvedovski. American Ceramic Society, Baltimore, MD, USA, 2006, pp. 37–44.

5. Hayun, S., Frage, N., Dariel, M. P., Zaretsky, E. and Ashuah, Y., Dynamic response of B4C–SiC ceramic composites. In *Ceramic Transactions, Ceramic Armor and Armor Systems II*, ed. E. Medvedovski. American Ceramic Society, Baltimore, MD, USA, 2006, pp. 147–156.
6. Hayun, S., Rittel, D., Frage, N. and Dariel, M. P., Static and dynamic mechanical properties of infiltrated B4C–Si composites. *Mater. Sci. Eng. A*, 2008, **487**, 405–409.

[7]. Hayun, S., Dub, S., Dariel, M. P. and Frage, N., The effect of carbon source on the microstructure and the mechanical properties of reaction bonded boron carbide. In *Ceramic Transactions, Advances in Sintering*, ed. E. A. Olevsky and R. Bordia. American Ceramice Society, Baltimore, MD USA, 2010.

8. Telle, R., Structure and properties of silicon-doped boron carbide. *NATO ASI Ser. E: Appl. Sci.*, 1990, **185**, 249–267.
9. Telle, R. and Petzow, G., Mechanisms in the liquid phase sintering of boron carbide with silicon based melts. *Mater. Sci. Monogr.*, 1987, **38A**, 961–973.
10. Gugel, E., Kieffer, R., Leimer, G. and Ettmayer, P., Ternary system boron–carbon–silicon. *Solid State Chem.*, 1972, **364**, 505–513.
11. Chen, L., Lengauer, W., Ettmayer, P., Dreyer, K., Daub, H. W. and Kassel, D., Fundamentals of liquid phase sintering for modern cermets and functionally graded cemented carbonitrides (FGCC). *Int. J. Refract. Met. Hard Mater.*, 2001, **18**, 307–322.
12. Andren, H. O., Microstructures of cemented carbides. *Mater. Des.*, 2001, **22**, 491–498.
13. Moskowitz, D. and Humenik, M., Cemented titanium carbide cutting tools. *Mod. Dev. Powder Met.*, 1966, **3**, 83–94.
14. Sigl, L. S. and Kleebe, H. J., Core/rim structure of liquid-phase-sintered silicon carbide. *J. Am. Ceram. Soc.*, 1993, **76**, 773–776.
15. Ekbom, L., Antonsson, T. and Ekbom, M., Computer simulation of solution and growth processes during the initial stage of liquid phase sintering of tungsten heavy metal. *Scand. J. Metall.*, 2005, **34**, 312–316.
16. Zheng, Y., Wang, S., You, M., Tan, H. and Xiong, W., Fabrication of nanocomposite Ti(C. N)-based cermet by spark plasma sintering. *Mater. Chem. Phys.*, 2005, **92**, 64–70.
17. Mortensen, A., Kinetics of densification by solution-reprecipitation. *Acta Mater.*, 1997, **45**, 749–758.
18. Eremenko, V. N., Naidich, Y. V. and Lavrinenko, I. A., *Liquid-Phase Sintering*. Consultants Bureau, New York, 1970, p. 75.
19. Sokolova, E. V., Frage, N. R., Gurevich, Y. G. and Chumanov, V. I., Titanium carbide interaction with steel R6M5. *Poroshk. Metall. (Kiev.)*, 1991, **1**, 68–72.
20. Stoessell, R. K., Reaction paths and equilibrium end-points in solid-solution aqueous-solution systems. *Comments. Geochim. Cosmochim. Acta*, 1992, **56**, 2555–2557.
21. Glynn, P. D. and Reardon, E. J., Solid-solution aqueous-solution equilibria: thermodynamic theory and representation. *Am. J. Sci.*, 1992, **292**, 215–225.
22. Nourtier-Mazauric, E., Guy, B., Fritz, B., Brosse, E., Garcia, D. and Clement, A., Modelling the dissolution/precipitation of ideal solid solutions. *Oil Gas Sci. Technol.*, 2005, **60**, 401–415.
23. Thorstenson, D. C. and Plummer, L. N., Equilibrium criteria for two-component solids reacting with fixed composition in an aqueous phase—example: the magnesian calcites. *Am. J. Sci.*, 1977, **277**, 1203–1223.
24. Frage, N., Levin, L. and Dariel, M. P., The effect of the sintering atmosphere on the densification of B4C ceramics. *J. Solid State Chem.*, 2004, **177**, 410–414.
25. Morosin, B., Aselage, T. L. and Feigelson, R. S., Crystal structure refinements of rhombohedral symmetry materials containing boron-rich icosahedra. *Mater. Res. Symp. Proc.*, 1987, **97**, 145–149.
26. Hayun, S., Weizmann, A., Dilman, H., Dariel, M. and Frage, P. N., Rim region growth and its composition in reaction bonded boron carbide composites with core-rim structure. *J. Phys. Conf. Ser.*, 2009, 176.
27. Werheit, H., Kuhlmann, U., Laux, M. and Telle, R., Solid solutions of silicon in boron-carbide-type crystals. *J. Alloys Compd.*, 1994, **209**, 181–188.
28. Goujard, S., Vandenbulcke, L., Bernard, C., Blondiaux, G. and Debrun, J. L., Thermodynamic and experimental study of the chemical vapor codeposition in the silicon–boron–carbon system at 1400 K. *J. Electrochem. Soc.*, 1994, **141**, 452–461.
29. Kasper, B., *Phasengleichgewichte im System B–C–N–Si*. Ph. D., University of Stuttgart, Germany, 1996.
30. Anonymous Thermocalc Software, Version Q. *Foundation of computational thermodynamics*. Stockholm, Sweden.
31. Panasyuk, A. D., Oreshkin, V. D. and Maslennikova, V. R., Kinetics of the reactions of boron carbide with liquid aluminum, silicon, nickel, and iron. *Powder Metall. Met. Ceram.*, 1979, **18**, 487–490.
32. Scace, R. I. and Slack, G. A., Solubility of carbon in silicon and germanium. *J. Chem. Phys.*, 1959, **30**, 1551–1555.
33. Ness, J. N. and Page, T. F., Microstructural evolution in reaction-bonded silicon carbide. *J. Mater. Sci.*, 1986, **21**, 1377–1397.
34. Li, J. and Hausner, H., Reactive wetting in the liquid–silicon/solid–carbon system. *J. Am. Ceram. Soc.*, 1996, **79**, 873–880.
35. Sawyer, G. R. and Page, T. F., Microstructural characterization of "REFEL" (reaction-bonded) silicon carbides. *J. Mater. Sci.*, 1978, **13**, 885–904.
36. Favre, A., Fuzellier, H. and Suptil, J., An original way to investigate the siliconizing of carbon materials. *Ceram. Int.*, 2003, **29**, 235–243.
37. Zollfrank, C. and Sieber, H., Microstructure evolution and reaction mechanism of biomorphous SiSiC ceramics. *J. Am. Ceram. Soc.*, 2005, **88**, 51–58.
38. Fitzer, E. and Gadow, R., Fiber-reinforced silicon carbide. *Am. Ceram. Soc. Bull.*, 1986, **65**, 326–335.
39. Moberlychan, W. J., Cao, J. J., Gilbert, C. J., Ritchie, R. O. and Joghe, L. C., The cubic to hexagonal transformation to toughen SiC. In *Proceedings of the International materials symposium on ceramic microstructures'96: control at the atomic level*, ed. A. P. Tomsia and A. M. Glaeser. Springer, Plenum Press, New York, 1998, pp. 177–190.
40. Pampuch, R., Bialoskorski, J. and Walasek, E., Mechanism of reactions in the $Si_l + C_f$ system and the self-propagating high-temperature synthesis of silicon carbide. *Ceram. Int.*, 1987, **13**, 63–68.